arXiv:1610.03578v1 [cond-mat.mtrl-sci] 12 Oct 2016

New p- and n-type ferromagnetic semiconductors: Cr-doped $BaZn_2As_2$

Bo Gu[1*] and Sadamichi Maekawa[1,2]
[1] *Advanced Science Research Center, Japan Atomic Energy Agency, Tokai 319-1195, Japan*
[2] *ERATO, Japan Science and Technology Agency, Sendai 980-8577, Japan*

(Dated: October 13, 2016)

We find new ferromagnetic semiconductors, Cr-doped $BaZn_2As_2$, by employing a combined method of the density functional theory and the quantum Monte Carlo simulation. Due to a narrow band gap of 0.2 eV in host $BaZn_2As_2$ and the different hybridization of 3d orbitals of Cr impurity, the impurity bound states have been induced both below the top of valence band and above the bottom of conduction band. The long-range ferromagnetic coupling between Cr impurities is obtained with both p- and n-type carriers.

PACS numbers: 75.50.Pp, 75.30.Hx, 02.70.Ss

I. INTRODUCTION

After the discovery of ferromagnetism in (Ga,Mn)As, diluted magnetic semiconductors (DMS) have received considerable attention owing to potential applications based on the use of both their charge and spin degrees of freedom in electronic devices[1,2]. The substitution of divalent Mn atoms into trivalent Ga sites introduces hole carriers; thus, (Ga,Mn)As is a p-type DMS. The valence mismatch between Mn and Ga leads to severely limited chemical solubility for Mn in GaAs. Moreover, owing to simultaneous doping of charge and spin induced by Mn substitution, it is difficult to optimize charge and spin densities at the same time. The highest Curie temperature of (Ga,Mn)As has been $T_c = 190$ K[3].

To overcome these difficulties, a new type of DMS, i.e., Li(Zn,Mn)As was proposed[4] and later fabricated with $T_c = 50$ K[5]. It is based on LiZnAs, a I−II−V semiconductor. Spin is introduced by isovalent (Zn^{2+}, Mn^{2+}) substitution, which is decoupled from carrier doping with excess/deficient Li concentration. Although Li(Zn,Mn)As was proposed as a promising n-type DMS with excess Li^+, p-type carriers were obtained in the experiment with excess Li. The introduction of holes was presumably because of the excess Li^+ in substitutional Zn^{2+} sites[5]. Later, another I−II−V DMS, i.e., Li(Zn,Mn)P was reported in an experiment with $T_c = 34$ K[6]. Li(Zn,Mn)P with excess Li was determined to be of p-type as well in the experiment. According to first-principles calculations, the reason for this is the same as that for Li(Zn,Mn)As[6]. Recently, a Cr-doped p-type I−II−V DMS, Li(Zn,Cr)As with T_c about 218 K has been reported in experiment[7], which is higher than that for (Ga,Mn)As.

Another type of DMS (Ba,K)$(Zn,Mn)_2As_2$ was observed in experiments with T_c up to 230 K[8,9], which is also higher than that for (Ga,Mn)As. Based on the semiconductor $BaZn_2As_2$, holes were doped by (Ba^{2+}, K^+) substitutions, and spins by isovalent (Zn^{2+}, Mn^{2+}) substitutions. It was a p-type DMS. Motivated by the high T_c, density functional theory (DFT) calculations[10] and photoemission spectroscopy experiments[11,12] were conducted to understand the microscopic mechanism of ferromagnetism of p-type DMS (Ba,K)$(Zn,Mn)_2As_2$. By contrast, an n-type DMS, i.e., $Ba(Zn,Mn,Co)_2As_2$ was recently reported in an experiment with $T_c \sim 80$ K[13]. In this material, electrons are doped because of the substitution of Zn with Co, and spins are generated mainly because of (Zn^{2+}, Mn^{2+}) substitutions. A recent quantum Monte Carlo simulation combined with DFT calculation has been carried out to study the mechanism of p- and n-type ferromagnetism in Mn-doped $BaZn_2As_2$[14].

Motivated by the high T_c reported in Cr-doped LiZnAs and Mn-doped $BaZn_2As_2$, here we study a new diluted magnetic semiconductor: Cr-doped $BaZn_2As_2$. By a combined method of the density function theory and quantum Monte Carlo simulation, we study the magnetic properties of Cr impurities in host $BaZn_2As_2$.

II. DFT+QMC METHOD

In the following, we calculate the electronic and magnetic properties of Cr-doped $BaZn_2As_2$ DMS, which has a narrow band gap Δ_g (= 0.2 eV)[8]. We use a combination of the DFT[15,16] and the Hirsch−Fye quantum Monte Carlo (QMC) simulation[17]. Our combined DFT+QMC method can be used for in-depth treatment of the band structures of materials and strong electron correlations of magnetic impurities on an equal footing; thus, it can be applied for designing new functional semiconductor-[14,18–20] and metal-based[21–23] materials. The method involves two calculations steps. First, the Haldane−Anderson impurity model[24] is formulated within the local density approximation for determining the host band structure and impurity-host hybridization. Second, magnetic correlations of the Haldane-Anderson impurity model at finite temperatures are calculated using the Hirsch−Fye QMC technique[17].

The Haldane−Anderson impurity model is defined as follows:

$$H = \sum_{\mathbf{k},\alpha,\sigma} [\epsilon_\alpha(\mathbf{k}) - \mu] c^\dagger_{\mathbf{k}\alpha\sigma} c_{\mathbf{k}\alpha\sigma} + \sum_{\mathbf{k},\alpha,\mathbf{i},\xi,\sigma} (V_{\mathbf{i}\xi\mathbf{k}\alpha} d^\dagger_{\mathbf{i}\xi\sigma} c_{\mathbf{k}\alpha\sigma} + h.c.) + (\epsilon_d - \mu) \sum_{\mathbf{i},\xi,\sigma} d^\dagger_{\mathbf{i}\xi\sigma} d_{\mathbf{i}\xi\sigma} + U \sum_{\mathbf{i},\xi} n_{\mathbf{i}\xi\uparrow} n_{\mathbf{i}\xi\downarrow}, \quad (1)$$

where $c^{\dagger}_{\mathbf{k}\alpha\sigma}$ ($c_{\mathbf{k}\alpha\sigma}$) is the creation (annihilation) operator for a host electron with wave vector $\mathbf{k}$ and spin σ in the valence band ($\alpha = v$) or the conduction band ($\alpha = c$), and $d^{\dagger}_{\mathbf{i}\xi\sigma}$ ($d_{\mathbf{i}\xi\sigma}$) is the creation (annihilation) operator for a localized electron at impurity site $\mathbf{i}$ in orbital ξ and spin σ with $n_{\mathbf{i}\xi\sigma} = d^{\dagger}_{\mathbf{i}\xi\sigma} d_{\mathbf{i}\xi\sigma}$. Here, $\epsilon_{\alpha}(\mathbf{k})$ is the host band dispersion, μ is the chemical potential, $V_{\mathbf{i}\xi\mathbf{k}\alpha}$ denotes hybridization between the impurity and the host, ϵ_d is the impurity $3d$ orbital energy, and U is the on-site Coulomb repulsion of the impurity. Considering the condition of Hund coupling $J_H \ll U$, J_H is neglected and the single-orbital approximation is used to describe the magnetic sates of impurities.

III. RESULTS FOR $Ba(Zn,Cr)_2As_2$

The parameters $\epsilon_{\alpha}(\mathbf{k})$ and $V_{\mathbf{i}\xi\mathbf{k}\alpha}$ are obtained by DFT calculations using the Wien2k package[25]. To reproduce the experimental narrow band gap of 0.2 eV in $BaZn_2As_2$[8], we use the modified Becke−Johnson exchange potential (mBJ)[26], which has been implemented in the Wien2k package. The obtained energy band ϵ_{α} ($\mathbf{k}$) is shown in Fig. 1 (a), where $BaZn_2As_2$ has space group I4/mmm. We obtained an indirect gap band $\Delta_g = 0.2$ eV, which is in good agreement with the experimental[8] and previous calculated[11,27] values.

The hybridization parameter between the ξ orbitals of a Cr impurity and $BaZn_2As_2$ host is defined as $V_{\mathbf{i}\xi\mathbf{k}\alpha} \equiv \langle\varphi_{\xi}(\mathbf{i})|H|\Psi_{\alpha}(\mathbf{k})\rangle \equiv \frac{1}{\sqrt{N}} e^{i\mathbf{k}\cdot\mathbf{i}} V_{\xi\alpha}(\mathbf{k})$, which can be expressed as

$$V_{\xi\alpha}(\mathbf{k}) = \sum_{o,\mathbf{n}} e^{i\mathbf{k}\cdot(\mathbf{n}-\mathbf{i})} a_{\alpha o}(\mathbf{k}) \langle\varphi_{\xi}(\mathbf{i})|H|\varphi_o(\mathbf{n})\rangle, \quad (2)$$

where $\varphi_{\xi}(\mathbf{i})$ is the impurity $3d$ state at site $\mathbf{i}$, and $\Psi_{\alpha}(\mathbf{k})$ is the host state with wave vector $\mathbf{k}$ and band index α, which is expanded by atomic orbitals $\varphi_o(\mathbf{n})$ having orbital index o and site index $\mathbf{n}$. Here, N is the total number of host lattice sites, and $a_{\alpha o}(\mathbf{k})$ is an expansion coefficient. To obtain the mixing integrals of $\langle\varphi_{\xi}(\mathbf{i})|H|\varphi_o(\mathbf{n})\rangle$, we consider a supercell $Ba_8Zn_{15}CrAs_{16}$, which comprises 2x2x2 primitive cells, where each primitive cell consists of a $BaZn_2As_2$, and a Zn atom is replaced by a Cr atom. The results of the hybridization function $V_{\xi\alpha}(\mathbf{k})$ are shown in Fig. 1 (b) for valence bands, and in 1 (c) for conduction bands.

The reasonable parameters U and ϵ_d for the Mn-doped $BaZn_2As_2$ are $U = 4$ eV and ϵ_d = -1.5 eV[14]. If we use these parameters for the Cr-doped $BaZn_2As_2$, Cr^{+} ($3d^5$) state is obtained by the QMC, while the isovalent (Zn^{2+}, Cr^{2+}) substitution was suggested by a recent experiment in Cr-doped LiZnAs[7]. In order to obtain Cr^{2+} ($3d^4$) state in the Cr-doped $BaZn_2As_2$ by the QMC, the reasonable parameters are $U = 4$ eV and ϵ_d = -1 eV. By the parameters obtained above, magnetic correlations of the impurities are calculated using the Hirsch−Fye QMC technique with more than 10^6 Monte Carlo sweeps and a Matsubara time step $\Delta\tau = 0.25$.

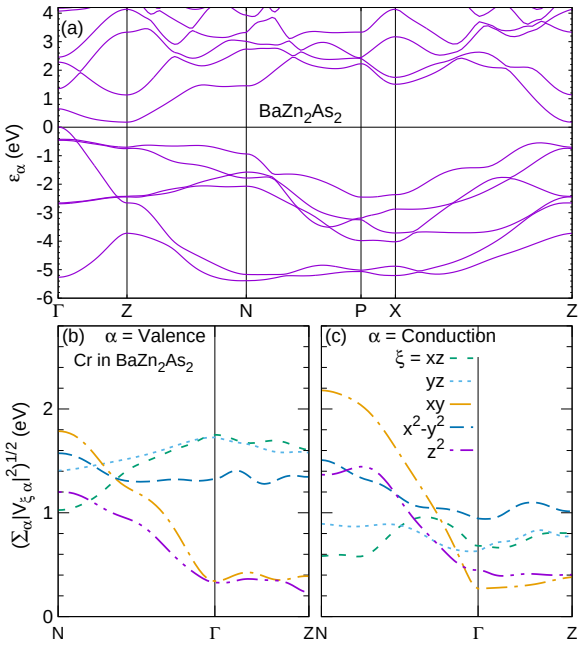

FIG. 1. Host band and hybridization parameters of Cr-doped $BaZn_2As_2$. (a) Energy bands ϵ_{α} of host $BaZn_2As_2$, which has space group I4/mmm. An indirect band gap of 0.2 eV was obtained by DFT calculations, which agrees well with the experimental value[8]. The hybridization function between the ξ orbitals of an Cr impurity and $BaZn_2As_2$ host (b) valence bands, and (c) conduction bands.

Figure 2 (a) shows a plot of the occupation number $\langle n_{\xi}\rangle$ of a ξ orbital of a Cr impurity in $BaZn_2As_2$ against the chemical potential μ at temperature 360 K. The top of the valence band (VB) was taken to be 0, and the bottom of the conduction band (CB) to be 0.2 eV. Operator n_{ξ} is defined as follows:

$$n_{\xi} = n_{\mathbf{i}\xi\uparrow} + n_{\mathbf{i}\xi\downarrow}. \quad (3)$$

The orbitals xz and yz of Cr subsitutional impurities at the Zn site degenerate owing to the crystal field of $BaZn_2As_2$, which has a group space of I4/mmm[8]. Sharp increases in n_{ξ} are observed around -0.4 and -0.2 and -0.1 and 0.2 eV for the orbitals $\xi = xy$ and z^2 and $x^2 - y^2$ and $xz(yz)$, respectively. This implies the existence of an impurity bound state (IBS) at this energy ω_{IBS}[14,18–20,28–30]. In order to make the IBS more clear, we show the partial density of state of a Cr impurity, $d\langle n_{\xi}\rangle/d\mu$ in Fig. 2 (b). The peaks in $d\langle n_{\xi}\rangle/d\mu$ correspond to the positions of IBS. Figure 2 (c) shows the magnetic correlation $\langle M^z_{1\xi} M^z_{2\xi}\rangle$ between the ξ orbitals of two Cr impurities with fixed distance R_{12} of the 1st nearest neighbor. The operator $M^z_{\mathbf{i}\xi}$ of the ξ orbital at impurity site $\mathbf{i}$ is defined as follows:

$$M^z_{\mathbf{i}\xi} = n_{\mathbf{i}\xi\uparrow} - n_{\mathbf{i}\xi\downarrow}. \quad (4)$$

For each ξ orbital, ferromagnetic (FM) coupling is obtained when the chemical potential μ is close to the IBS

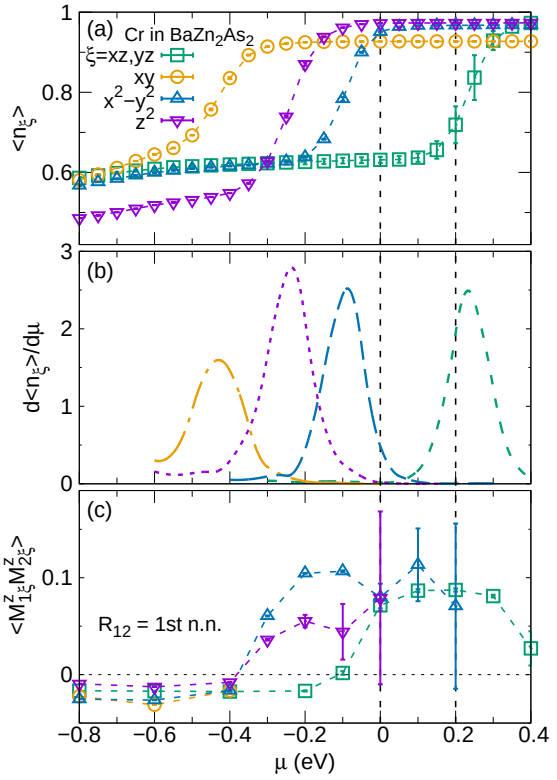

FIG. 2. For Cr-doped $BaZn_2As_2$, chemical potential μ dependence of (a) occupation number $\langle n_\xi \rangle$ of ξ orbital of a Cr impurity, (b) partial density of state $d\langle n_\xi \rangle / d\mu$, and (c) magnetic correlation $\langle M^z_{1\xi} M^z_{2\xi} \rangle$ between the ξ orbitals of two Cr impurities with fixed distance R_{12} of the 1st nearest neighbor, where the temperature is 360 K. The top of valence band is 0, and the bottom of conduction band is 0.2 eV.

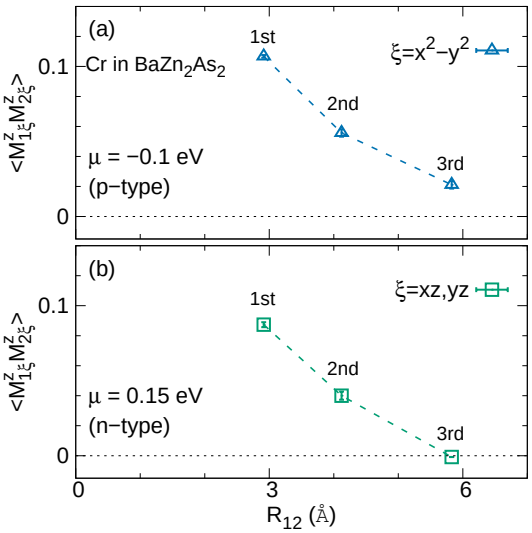

FIG. 3. For Cr-doped $BaZn_2As_2$, the distance R_{12} dependence of magnetic correlation $\langle M^z_{1\xi} M^z_{2\xi} \rangle$ between the ξ orbitals of two Cr impurities for (a) p-type case with chemical potential μ = -0.1 eV and (b) n-type case with μ = 0.15 eV, where temperature is 360 K. The 1st, 2nd, and 3rd nearest neighbors of R_{12} are noted.

position, and FM correlations become weaker and eventually disappear when μ moves away from the IBS. This role of the IBS in determining the strength of FM correlations between impurities corresponds to the picture of carrier-mediated FM coupling, which has been discussed in various DMS systems[14,18–20,28–30].

For Cr-doped $BaZn_2As_2$ with p-type carriers, we take μ = -0.1 eV as an estimate for the p-type case, which is below the top of VB by 0.1 eV. Figure 3 (a) shows the distance R_{12} dependence of the magnetic correlation $\langle M^z_{1\xi} M^z_{2\xi} \rangle$ between the ξ orbitals of two Cr impurities with μ = -0.1 eV. Long-range FM coupling up to approximately 6 Å(the 3rd nearest neighbor) is obtained for the orbital $\xi = x^2 - y^2$, while no longe-range FM coupling is obtained for the other orbitals.

For Cr-doped $BaZn_2As_2$ with n-type carriers, we take μ = 0.15 eV as an estimate for the n-type case, which is below the bottom of CB by 0.05 eV. As shown in Fig. 3 (b), long-range FM coupling up to approximately 6 Å(the 3rd nearest neighbor) is obtained for the orbitals $\xi = xz$ and yz. No FM is obtained for the other three orbitals, shown in Fig. 2 (b) as well. A Comparison of Figs. 3 (a) and (b) shows that the magnitude of FM coupling $\langle M^z_{1\xi} M^z_{2\xi} \rangle$ in the n-type case is slightly smaller than that in the p-type case.

IV. DISCUSSION

Here, we discuss that the microscopic pictures of the FM coupling in the Cr- and Mn-doped $BaZn_2As_2$ are different. As shown in Fig. 4(a), the position of IBS for orbital ξ (xz, yz) is near the bottom of CB for the Cr impurity, while it is near the top of VB for the Mn impurity[14]. This is because the impurity level of Cr is higher than that of Mn. As shown in Fig. 4(b), the FM correlation $\langle M^z_{1\xi} M^z_{2\xi} \rangle$ between the orbital ξ (xz, yz) of two impurities with the 1st nearest neighbor is developed when the chemical potential μ is around the bottom of CB for the Cr impurity, while the FM correlation is developed when μ is around the top of VB for the Mn impurity. As a result, for the p-type carrier with μ = -0.1 eV, the FM correlation between the orbital ξ (xz, yz) is obtained for the Mn impurity, while nonmagnetic correlation between the orbital ξ (xz, yz) is obtained for the Cr impurity. For the n-type carrier with $\mu \sim 0.2$ eV, the FM correlation for the Cr impurity is more promising than that for the Mn impurity, which is indicated by the IBS near the bottom of CB for the Cr impurity in Fig. 4(a) as well as by the larger error bars in the FM correlation for the Mn impurity in Fig. 4(b).

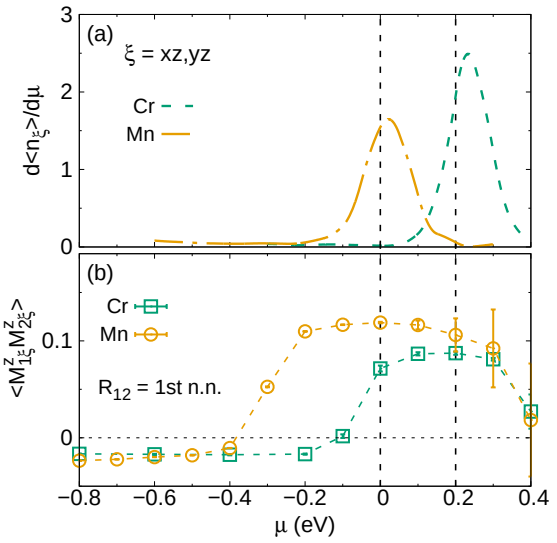

FIG. 4. Comparison between the Cr- and Mn-doped $BaZn_2As_2$. Chemical potential μ dependence of (a) partial density of state $d\langle n_\xi\rangle/d\mu$, and (b) magnetic correlation $\langle M^z_{1\xi}M^z_{2\xi}\rangle$ between the ξ (xz, yz) orbitals of two impurities with the 1st nearest neighbor.

V. CONCLUSIONS

In summary, we find new ferromagnetic semiconductors, Cr-doped $BaZn_2As_2$, by employing a combined method of the density function theory and quantum Monte Carlo simulation. Due to a narrow band gap of 0.2 eV in host $BaZn_2As_2$ and the different hybridization of 3d orbitals of Cr impurity, the impurity bound states have been induced close to the top of valence band as well as the bottom of conduction band. As a result, the long-range ferromagnetic coupling between Cr impurities is obtained with both p- and n-type carriers.

ACKNOWLEDGMENTS

The authors acknowledge H. Y. Man, F. L. Ning, C. Q. Jin, H. Suzuki, and A. Fujimori for many valuable discussions on the experiments of DMS.

* Corresponding author: gu.bo@jaea.go.jp

[1] H. Ohno, Science **281**, 951 (1998).
[2] T. Dietl, Nat. Mater. **9**, 965 (2010).
[3] M. Wang, R. P. Campion, A. W. Rushforth, K. W. Edmonds, C. T. Foxon, and B. L. Gallagher, Appl. Phys. Lett. **93**, 132103 (2008).
[4] J. Masek, J. Kudrnovsky, F. Maca, B. L. Gallagher, R. P. Campion, D. H. Gregory, and T. Jungwirth, Phys. Rev. Lett. **98**, 067202 (2007).
[5] Z. Deng et al., Nat. Commun. **2**, 422 (2011).
[6] Z. Deng et al., Phys. Rev. B **88**, 081203(R) (2013).
[7] Q. Wang, H. Man, C. Ding, X. Gong, S. Guo, H. Jin, H. Wang, B. Chen, and F. L. Ning, J. Appl. Phys. **115**, 083917 (2014).
[8] K. Zhao et al., Nat. Commun. **4**, 1442 (2013).
[9] K. Zhao, B. J. Chen, G. Q. Zhao, Z. Yuan, Q. Q. Liu, Z. Deng, J. L. Zhu, and C. Q. Jin, Chin. Sci. Bull. **59**, 2524 (2014).
[10] J. K. Glasbrenner, I. Zutic, and I. I. Mazin, Phys. Rev. B **90**, 140403(R) (2014).
[11] H. Suzuki et al., Phys. Rev. B **91**, 140401(R) (2015).
[12] H. Suzuki et al., Phys. Rev. B **92**, 235120 (2015).
[13] H. Y. Man, C. Ding, S. L. Guo, G. X. Zhi, X. Gong, Q. Wang, H. D. Wang, B. Chen, and F. L. Ning, arXiv:1403.4019.
[14] B. Gu, and S. Maekawa, Phys. Rev. B **94**, 155202 (2016).
[15] P. Hohenberg and W. Kohn, Phys. Rev. **136**, B864 (1964).
[16] W. Kohn and L. J. Sham, Phys. Rev. **140**, A1133 (1965).
[17] J. E. Hirsch and R. M. Fye, Phys. Rev. Lett. **56**, 2521 (1986).
[18] B. Gu, N. Bulut, and S. Maekawa, J. Appl. Phys. **104**, 103906 (2008).
[19] J. Ohe, Y. Tomoda, N. Bulut, R. Arita, K. Nakamura, and S. Maekawa, J. Phys. Soc. Jpn. **78**, 083703 (2009).
[20] B. Gu, N. Bulut, T. Ziman, and S. Maekawa, Phys. Rev. B **79**, 024407 (2009).
[21] B. Gu, J. Y. Gan, N. Bulut, T. Ziman, G. Y. Guo, N. Nagaosa, and S. Maekawa, Phys. Rev. Lett. **105**, 086401 (2010).
[22] B. Gu, I. Sugai, T. Ziman, G. Y. Guo, N. Nagaosa, T. Seki, K. Takanashi, and S. Maekawa, Phys. Rev. Lett. **105**, 216401 (2010).
[23] Z. Xu, B. Gu, M. Mori, T. Ziman, and S. Maekawa, Phys. Rev. Lett. **114**, 017202 (2015).
[24] F. D. M. Haldane and P. W. Anderson, Phys. Rev. B **13**, 2553 (1976).
[25] P. Blaha, K. Schwart, G. K. H. Hadsen, D. Kvasnicka, and J. Luitz, WIEN2K, An Augmented Plane Wave Plus Local Orbitals Program for Calculating Crystal Properties, Vienna University of Technology, Vienna, 2001.
[26] F. Tran and P. Blaha, Phys. Rev. B **83**, 235118 (2011).
[27] I. R. Shein and A. L. Ivanovskii, J. Alloys Compd. **583**, 100 (2014).
[28] M. Ichimura, K. Tanikawa, S. Takahashi, G. Baskaran, and S. Maekawa, *Foundations of Quantum Mechanics in the Light of New Technology*, edited by S. Ishioka and K. Fujikawa. (World Scientific, Singapore, 2006), pp. 183-186.
[29] N. Bulut, K. Tanikawa, S. Takahashi, and S. Maekawa, Phys. Rev. B **76**, 045220 (2007).
[30] Y. Tomoda, N. Bulut, and S. Maekawa, Physica B **404**, 1159 (2009).